THE ASTROPHYSICAL JOURNAL, 399:134–146, 1992 November 1

INFRARED SPECTROSCOPY OF DENSE CLOUDS IN THE C–H STRETCH REGION: METHANOL AND "DIAMONDS"

L. J. ALLAMANDOLA,[1] S. A. SANDFORD,[1] AND A. G. G. M. TIELENS
NASA Ames Research Center, MS 245-6, Mountain View, CA 94035

AND

T. M. HERBST
Institute for Astronomy, 2680 Woodlawn Drive, University of Hawaii, Honolulu, HI 96822
Received 1991 September 3; accepted 1992 April 30

ABSTRACT

High spectral resolution ($\nu/\Delta\nu = 900$) studies in the 3100–2600 cm^{-1} (3.2–3.9 μm) range are presented of the protostars NGC 7538 IRS 9, W33A, W3 IRS 5, and S140 IRS 1. This is the spectral region in which the fundamental C–H stretching vibrations of aliphatic hydrocarbons fall. Well-resolved absorption bands at about 2825 cm^{-1} (3.54 μm) and 2880 cm^{-1} (3.47 μm) were found superposed on the low-frequency wing of the strong O–H stretch feature. The 2880 cm^{-1} (3.47 μm) band, a new interstellar feature, is moderately strong in the spectra of all four objects studied. The 2825 cm^{-1} (3.54 μm) band, previously detected toward W33A, is also in the spectrum of NGC 7538 IRS 9. The relative strength of these two bands varies, showing that they are associated with two different carriers.

On the basis of comparisons with laboratory spectra, the 2825 cm^{-1} (3.54 μm) band is assigned to methanol (CH_3OH), in agreement with the earlier work of Grim et al. (1991). This assignment is further supported by a pair of weak absorptions centered at 2600 and 2540 cm^{-1} (3.85 and 3.94 μm) in the spectrum of W33A recently reported by Geballe (1991). These features compare very well with laboratory spectra of CH_3OH/H_2O ice mixtures. The CH_3OH/H_2O ratio derived from the 2825 cm^{-1} methanol band and the 3250 cm^{-1} (3.08 μm) H_2O feature are 0.13 and 0.40 for NGC 7538 IRS 9 and W33A, respectively. These values are smaller than the ratios of 0.61 and 0.54 derived using the 1460 cm^{-1} (6.85 μm) band assigned to CH_3OH and the 1665 cm^{-1} (6.00 μm) H_2O band. These apparent discrepancies may be due to a combination of scattering effects within the molecular cloud, uncertainties associated with the baselines for the 2825 cm^{-1} feature, and the presence of other interstellar grain materials that absorb at 1460 cm^{-1} (6.85 μm). Nonetheless, after H_2O, CH_3OH is the most abundant known interstellar ice constituent.

The new band at about 2880 cm^{-1} (3.47 μm) falls near the position for C–H stretching vibrations in tertiary carbon atoms $\left(-\overset{|}{\underset{|}{C}}H\right)$. The strength of this feature, in combination with the lack of strong features associated with primary ($-CH_3$) and secondary ($-CH_2-$) carbon atoms, suggests that the carrier of the new feature has a diamond-like structure. We therefore tentatively attribute this new feature to interstellar "diamonds." The detection of this band in the spectra of all four dense molecular clouds suggests that the carrier is ubiquitous in dense clouds. Band-strength analysis indicates that a minimum of a few percent of the available cosmic carbon is tied up in this material.

Subject headings: H II regions — infrared: interstellar: lines — ISM: molecules — line: identification

1. INTRODUCTION

In this paper we discuss observations made in the 3100–2600 cm^{-1} (3.2–3.9 μm) spectral region to place constraints on the hydrocarbon component of dust in dense interstellar molecular clouds. A wing on the low-frequency side of the 3250 cm^{-1} (3.08 μm) ice feature is evident in the spectra of many infrared sources embedded in these clouds (Willner et al. 1982; Whittet et al. 1983; Eiroa et al. 1987; Smith, Sellgren, & Tokunaga 1987, 1989; Tanaka et al. 1990; Hough et al. 1988). Various suggestions have been made to account for this wing. It may arise from a combination of many overlapping aliphatic C–H stretching bands, hydrogen bonding between the H_2O and other strongly basic mantle components such as NH_3 (Hagen, Tielens, & Greenberg 1983; Allamandola 1984), and scattering from large grains (Léger et al. 1983). This subject is reviewed in Tielens (1989).

Weak absorptions characteristic of aliphatic C–H stretching vibrations have long been expected to be superposed on the low-frequency wing of the 3250 cm^{-1} (3.08 μm) O–H feature (Hagen, Allamandola, & Greenberg 1980; Allamandola 1984; Tielens et al. 1984; Tielens & Allamandola 1987). Although severely blended with the strong H_2O ice band and wing, a high-resolution spectral search for these features is warranted because their peak frequencies and relative strengths are characteristic of specific molecules and chemical classes and they have the potential to reveal much about the chemistry of the interstellar medium (ISM). In addition to searching for unexpected new bands which would provide further insight into the carbonaceous component of interstellar dust and ices, these

[1] Visiting Astronomer, Infrared Telescope Facility, which is operated by the University of Hawaii under contract with the National Aeronautics and Space Administration.

measurements also serve as a test of the initial assignment of the 1460 cm^{-1} (6.85 μm) band to CH_3OH (Tielens & Allamandola 1987) and probe for H_2CO, a molecule predicted to be present in much higher abundances in grains than are found (Tielens & Hagen 1982; d'Hendecourt, Allamandola, & Greenberg 1985). This region is particularly well suited for the latter two goals. Methanol has a unique absorption at 2828 cm^{-1} (3.536 μm) and H_2CO has two characteristic bands of nearly equal strength at 2853 and 2785 cm^{-1} (3.505 and 3.591 μm) when frozen in H_2O ice (d'Hendecourt & Allamandola 1986; van der Zwet et al. 1985).

The spectrum of W33A measured between 2940 and 2740 cm^{-1} (3.40 and 3.65 μm) revealed a new band at 2825 cm^{-1}, supporting the methanol assignment but raising important questions regarding its abundance with respect to H_2O (Baas et al. 1988; Grim et al. 1991). They derive $CH_3OH/H_2O = 0.07$ from a comparison of the strength of the 2825 cm^{-1} CH_3OH and 1660 cm^{-1} H_2O bands in W33A. Since this is significantly lower than the value of 0.55 deduced by comparing the 1460 cm^{-1} (6.85 μm) CH_3OH band with the 1660 cm^{-1} H_2O band (Tielens & Allamandola 1987), they propose that the 1460 cm^{-1} (6.85 μm) band is mainly due to another species, possibly NH_4^+. Recently the 1026 cm^{-1} (9.7 μm) C–O stretching mode and the 1128 cm^{-1} (8.9 μm) $-CH_3$ rocking mode of CH_3OH have been detected toward the protostar GL 2136 (Skinner et al. 1992). While the peak position of the 1026 cm^{-1} band implies a CH_3OH/H_2O ratio in excess of 0.5, comparison of the CH_3OH column densities with that of H_2O implies a ratio of only 0.05. Possibly, the CH_3OH is located in an independent ice component which represents only a fraction of the grains along the line of sight. Observational searches for the CH_3OH 1026 cm^{-1} (9.7 μm) band toward AFGL 961, AFGL 2591, the BN object, and Mon R2 No. 3 have placed very conservative upper limits to CH_3OH on the order of 10%–20% of the H_2O in these clouds (Schutte, Tielens, & Sandford 1991).

The results of high-resolution spectroscopic observations of NGC 7538 IRS 9, W33A, W3 IRS 5, and S140 IRS 1 from 3125 to 2630 cm^{-1} (3.2–3.8 μm) are presented here. These spectra confirm the methanol assignment and put lower limits on the abundance of methanol present in ice mantles. The spectra also put upper limits on the abundance of formaldehyde and reveal a new absorption feature. The new band suggests the apparent ubiquity of interstellar tertiary carbon, i.e., interstellar "diamonds," in dense molecular clouds. The observations and a brief description of each object are presented in §§ 2 and 3. These are followed by analysis of the spectra and detailed discussion in § 4.

2. OBSERVATIONS AND DATA REDUCTION

All the observations reported here were made using the 3-m telescope at the NASA Infrared Telescope Facility (IRTF) on Mauna Kea. The spectra were measured using the 32 InSb detector, LN_2-cooled, Cooled-Grating Array Spectrometer (CGAS). The performance and configuration of this instrument are described in more detail elsewhere (Tokunaga, Smith, & Irwin 1987). Detectors 1, 2, 13, and 32 did not work reliably on the CGAS, and the output from these detectors was not used. We used grating A, which has 75 grooves mm^{-1} and provides a resolving power of about 180 over the 3500–2800 cm^{-1} (2.8–3.6 μm) range, and grating B, which has 300 grooves mm^{-1} and provides a resolving power of about 900 over the 3100–2600 cm^{-1} (3.2–3.8 μm) range. Both gratings were used in first order. Wavelength calibration was achieved in second order by comparison with the 5901 cm^{-1} (1.695 μm) line of an argon lamp. The detector spacing on the CGAS provides one detector per resolution element. The CGAS has a fixed aperture of 2".7 diameter.

We observed NGC 7538 IRS 9 using grating B on 1989 August 8 and grating A on 1989 August 9. The objects W33A, W3 IRS 5, and S140 IRS 1 were observed using grating B on the nights of 1990 September 4, 5, and 6. The observations of NGC 7538 IRS 9 were made using an order-sorting filter which had a bandpass of 4150–1175 cm^{-1} (2.41–8.51 μm). The other objects were observed using a filter with a bandpass of 3300–1250 cm^{-1}(3.0–8.0 μm).

Sky subtraction was accomplished by alternately measuring the object and nearby sky by nodding the telescope. Correction for atmospheric absorption was accomplished by comparison with nearby bright stars whose spectra were measured through similar air masses on the same night immediately before or after the object was observed. No further extinction corrections were made to the data, since, with the exception of W33A, the average air masses of the objects and their comparison stars differ by no more than 0.1 air masses (<0.03 air masses for NGC 7538 IRS 9). W33A differs in that several of the grating settings had considerably larger air-mass differences. This causes the most difficulty in the 3100–2950 cm^{-1} (3.2–3.4 μm) region, where telluric methane produces a strong set of absorption features.

The comparison stars were also used to determine the spectral shape of the objects. If we denote the measured (raw) spectrum of an object by $F(\lambda)$ and the measured comparison star spectrum by $S(\lambda)$, and if we assume that the comparison star spectrum can be characterized by a blackbody $B(\lambda, T)$ over the spectral range of interest, then the true spectrum of the object, $G(\lambda)$, is

$$G(\lambda) = \frac{F(\lambda)B(\lambda, T)}{S(\lambda)}, \quad (1)$$

where T is the color temperature of the comparison star near 3.45 μm.

Several pertinent parameters of the objects and comparison stars we studied are summarized in Table 1. The table lists the color temperatures and L-magnitudes derived for the compari-

TABLE 1

SUMMARY OF OBSERVATIONS

Object	Object R.A. (1950)	Object Decl. (1950)	Comparison Star and Spectral Type	Comparison Star Color Temperature (K)	Comparison Star L-Magnitude	Throw
NGC 7538 IRS 9	$23^h11^m52^s.7$	+61°10′30″.7	...	...	...	...
Grating A	...	...	BS 8854 (B0 Vn)	26500	6.15	180″ N-S
Grating B	...	...	BS 8926 (B3 IV)	15500	5.44	180″ N-S
W33A	18 11 44.2	−17 52 59.1	BS 6561 (F0 IV)	7030	2.68	60″ N-S
W3IRS 5	02 21 53.2	+61 52 21	BS 915 (G8 III+A2 V)	5000	0.66	60″ N-S
S140 IRS 1	22 17 41.3	+63 03 40	BS 8571	6000	2.40	60″ N-S

son stars. Fluxes are based on a 0.0 mag flux of 7.3×10^{-11} W m^{-2} μm^{-1} (IRTF Photometry Manual 1988). The comparison star spectra were also cross-compared with spectra from other bright stars observed during the same nights to ensure that none of the spectral features reported here are due to features within the comparison star spectra themselves. As a final precaution, comparisons were made between the spectra of several of the comparison stars at both high and low air masses in order to determine the behavior of telluric features in this spectral region. These comparisons were particularly important for interpreting the interference due to atmospheric methane in the spectrum of W33A.

3. THE OBJECTS AND SPECTRA

3.1. *Description of the Objects Studied*

The objects NGC 7538 IRS 9, W33A, W3 IRS 5, and S140 IRS 1 were chosen because they have all been well studied, they have high levels of extinction from dust in dense molecular clouds, and they all exhibit infrared spectra with molecular ice features. Furthermore, the spectra of NGC 7538 IRS 9, W33A, and W3 IRS 5 show the distince 1460 cm^{-1} (6.85 μm) band which has been attributed to CH_3OH (Tielens & Allamandola 1987). S140 IRS 1 also shows absorption in this region (Willner et al. 1982).

Of the many infrared sources in NGC 7538, IRS 9 is thought to be a protostellar object deeply embedded in a dense molecular cloud with an associated infrared reflection nebula (Werner et al. 1979). The source appears bipolar, with a dust torus around IRS 9 (Eiroa, Lenzen, & Gomez 1988). The optical depth of the 1030 cm^{-1} (9.6 μm) silicate band is 4.5 (Willner et al. 1982). Assuming $A_V/\tau = 18.6$ results in an estimate of $A_V = 84$, the value we adopt here. However, other determinations yield values which are half as large (Eiroa et al. 1988).

W33A is also thought to be a protostar deeply embedded in a dense molecular cloud (Capps, Gillett, & Knacke 1978). Although there is no evidence for a bipolar outflow, this object appears extended at 2 μm. The optical depth of the silicate band is 7.8 (Willner et al. 1982), which, assuming $A_V/\tau = 18.6$, implies an A_V of 145, the value we adopt here. Published A_V estimates for this object span the range from about 50 to slightly over 150 (Capps et al. 1978).

W3 IRS 5 and S140 IRS 1 (also called AFGL 2884) are also believed to be deeply embedded protostellar objects, and both have bipolar outflows. For W3 IRS 5 the silicate optical depth is 7.6 (Willner et al. 1982), implying $A_V = 142$. The silicate optical depth is 4 for S140 IRS 1 (Willner et al. 1982), implying $A_V = 74$. There is some evidence that S140 IRS 1 is also associated with an extended 2.2 μm reflection nebula (Dyck & Howell 1982).

In summary, all four objects are protostars deeply embedded inside dense molecular clouds. From the observed 10 μm silicate optical depth, visual extinctions ranging from 70 to 150 are deduced. However, because of complicated radiation transfer effects, these estimates are uncertain. It is likely that all objects have associated IR reflection nebula.

3.2. *The Spectra*

The low-resolution spectrum of NGC 7538 IRS 9 is shown in Figure 1. High-resolution spectra of NGC 7538 IRS 9, W33A, W3 IRS 5, and S140 IRS 1 are presented in Figure 2. All spectra have weak absorption features superposed on the low-frequency wing of the strong O–H stretching band which extends from about 3125 to 2670 cm^{-1} (3.20–3.75 μm). Figure 3 presents the 3000–2700 cm^{-1} (3.3–3.7 μm) region of these spectra replotted in absorbance (optical depth). The choice of baselines is not straightforward because they are difficult to define uniquely. For NGC 7538 IRS 9, W3 IRS 5, and S140 IRS 1 the lines shown in the linear flux plots of Figure 2 were used. The baseline endpoints were chosen to be 3000 and 2770 cm^{-1} (3.33 and 3.61 μm), the apparent limits to the broad absorption feature evident in the spectrum of NGC 7538 IR5 9 (our best spectrum). These linear baselines are probably reasonable approximations to the local continuum appropriate for these weak features, since they are substantially narrower than the underlying low-frequency wing. For W33A the linear baseline drawn on the logarithmic flux plot in Figure 2 was used, utilizing the same endpoints as for the other objects. Constructing a linear baseline on a linear flux plot is precluded for W33A because of the extreme depth of the solid O–H stretch band. For this reason, this baseline is probably the most uncertain of all for the objects studied here, and therefore most of the discussion of these spectra focuses on the other objects.

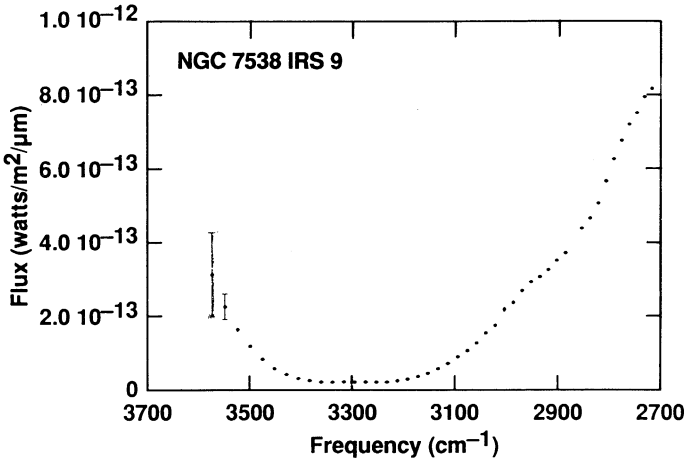

FIG. 1.—Low-resolution ($\nu/\Delta\nu \sim 180$ at 3000 cm^{-1}) spectrum between 3600 and 2700 cm^{-1} (2.8–3.7 μm) of the protostellar object NGC 7538 IRS 9. This region spans the range in which N–H, O–H, and C–H stretching vibrations fall. The error bars shown in this and subsequent figures represent $\pm 1\ \sigma$.

4. DISCUSSION

The spectra in Figures 1 and 2 have a broad, shallow, absorption from about 2980 to 2780 cm^{-1} (3.36–3.60 μm) with structure that varies from object to object. This absorption falls in the region where the fundamental C–H stretching vibrations occur for aliphatic hydrocarbons, i.e., hydrocarbon groups in which the carbon atom is singly bonded to the other atoms $\left(-CH_3,\ -CH_2-,\ -\underset{|}{\overset{|}{C}}H\right)$. The spectra of NGC 7538 IRS 9 and W33A have two resolved features which peak at about 2825 and 2880 cm^{-1} (3.54 and 3.47 μm), while the spectra of W3 IRS 5 and S140 IRS 1 show only a strong 2880 cm^{-1} (3.47 μm) band (Fig. 3). This variation implies that these features are associated with two independent components. The nature of these two components and the amount of interstellar material they represent are discussed in §§ 4.1–4.3.

4.1. *The 2825 cm^{-1} (3.54 μm) Band and Identification with Methanol*

The positions and widths of the interstellar 2825 and 2880 cm^{-1} (3.54 and 3.47 μm) features, as well as their absorp-

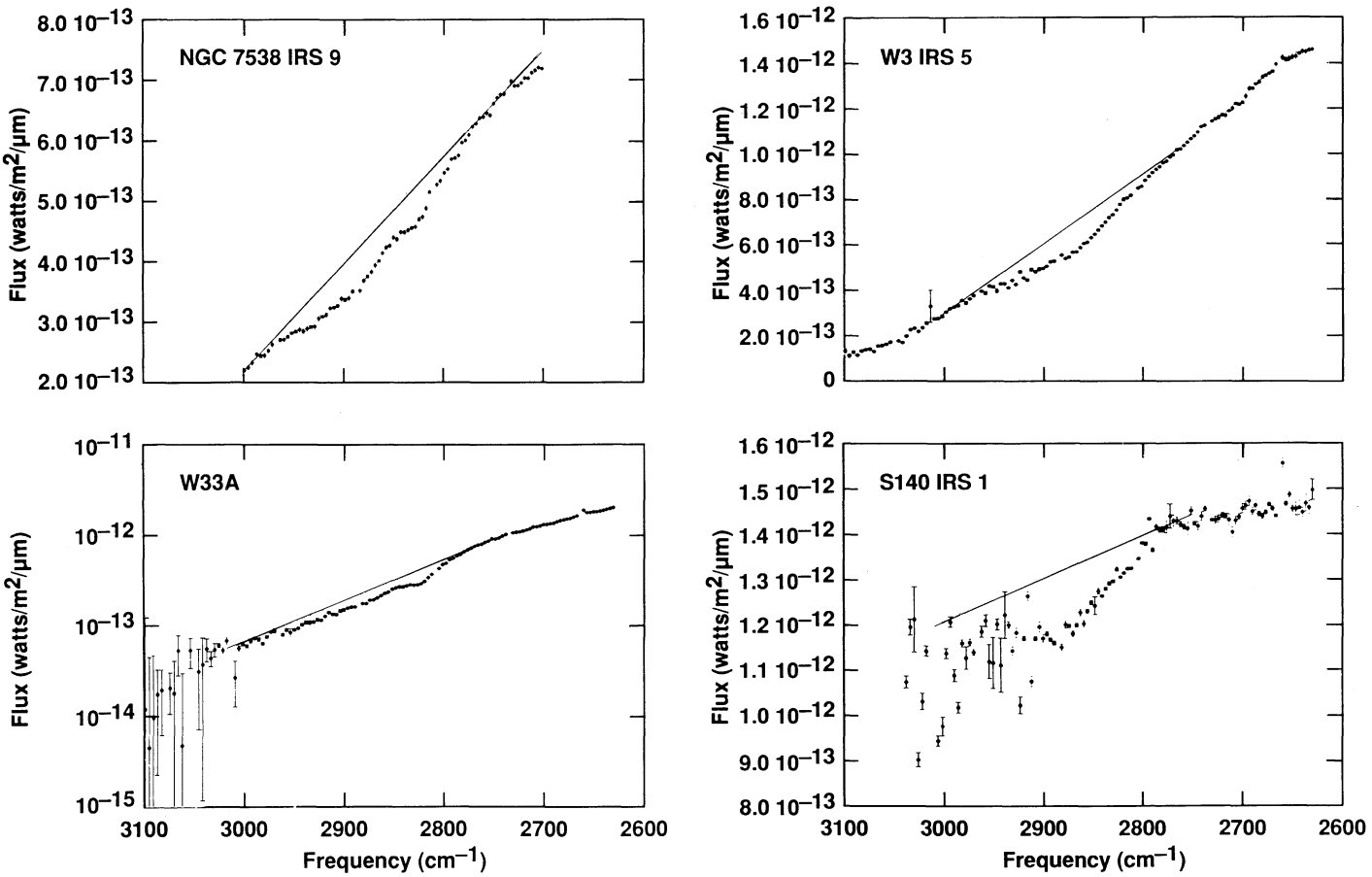

FIG. 2.—High-resolution ($\nu/\Delta\nu \sim 800$ at 3000 cm^{-1}) spectra in the C–H stretching region of the protostellar objects NGC 7538 IRS 9, W33A, W3 IRS 5, and S140 IRS 1. The line in each spectrum represents the baseline used to make the absorbance plots shown in subsequent figures.

tion strengths, place strong constraints on the types of molecules responsible. Figure 4 is illustrative of the spectral characteristics of *all* pure, saturated hydrocarbons [such as *n*-pentane (H_3C–CH_2–CH_2–CH_2–CH_3) and *n*-hexane (H_3C–CH_2–CH_2–CH_2–CH_2–CH_3)] in the C–H stretch region, namely, that the $-CH_3$ (methyl) asymmetric and symmetric C–H stretching modes fall at 2960 and 2870 cm^{-1} (3.38 and 3.48 μm), respectively, while the corresponding vibrations for the $-CH_2-$ (methylene) group occur at 2920 and 2860 cm^{-1} (3.43 and 3.50 μm). The integrated absorbance strengths of the asymmetric bands are comparable for the two groups, and about 2–3 times larger than that of the symmetric bands. In the interstellar spectra, *the absence of clearly discernible structure near* 2870 *and* 2860 cm^{-1} (3.48 *and* 3.50 μm), *as well as the lack of bands which are 2–3 times stronger near* 2960 *and* 2920 cm^{-1} (3.38 *and* 3.43 μm), *implies that pure saturated hydrocarbons are not responsible for the weak absorption features on the low-frequency wing of the interstellar* O–H *stretch band. This is in direct contrast to that found for dust in the diffuse interstellar medium* (Sandford et al. 1991).

The spectral properties of aliphatic groups ($-CH_3$, $-CH_2-$, $-\overset{|}{C}H$) in simple alcohols differs markedly from those of pure, saturated aliphatic hydrocarbons (Fig. 5). This is because the OH group substantially alters the adjacent molecular force field and bond strengths (see, e.g., Morrison & Boyd 1966). This influence of the OH group on the properties of a particular $-CH_3$, $-CH_2-$, and $-\overset{|}{C}H$ group comprising the same molecule diminishes with distance. Consequently, as the aliphatic hydrocarbon chain length of an alcohol increases, its spectrum begins to resemble that of a pure aliphatic hydrocarbon (see the octanol spectrum in Fig. 5). Methanol (CH_3OH), the simplest alcohol, is most affected (Fig. 5). Thus, spectroscopy in the C–H stretch region is an excellent way in which to test the methanol assignment further.

Figure 6 shows that there is excellent agreement between the 2828 cm^{-1} (3.536 μm) solid methanol band of a laboratory ice and those in NGC 7538 IRS 9 and W33A, and that the broader 3000–2900 cm^{-1} (3.33–3.45 μm) CH_3OH feature may contribute to the absorption at the high-frequency end of the broad interstellar feature centered at about 2880 cm^{-1} (3.47 μm). *This match confirms that methanol is frozen on the grains along the line of sight to these two objects.*

Further support of the methanol assignment toward W33A comes from the weak pair of absorption bands at about 2600 and 2540 cm^{-1} (3.85 and 3.94 μm) reported by Geballe (1991) and reproduced in Figure 7*a*. The profile of this band pair is compared with that of laboratory samples at 10 K of pure CH_3OH ice and CH_3OH in an H_2O:CH_3OH:CO:NH_3 = 100:50:1:1 ice mixture in Figures 7*b* and 7*c*. The good match in peak positions and overall profile to those of methanol ice shows that these weak bands are due to methanol. The better fit to the spectrum in Figure 7*c* suggests that the CH_3OH is

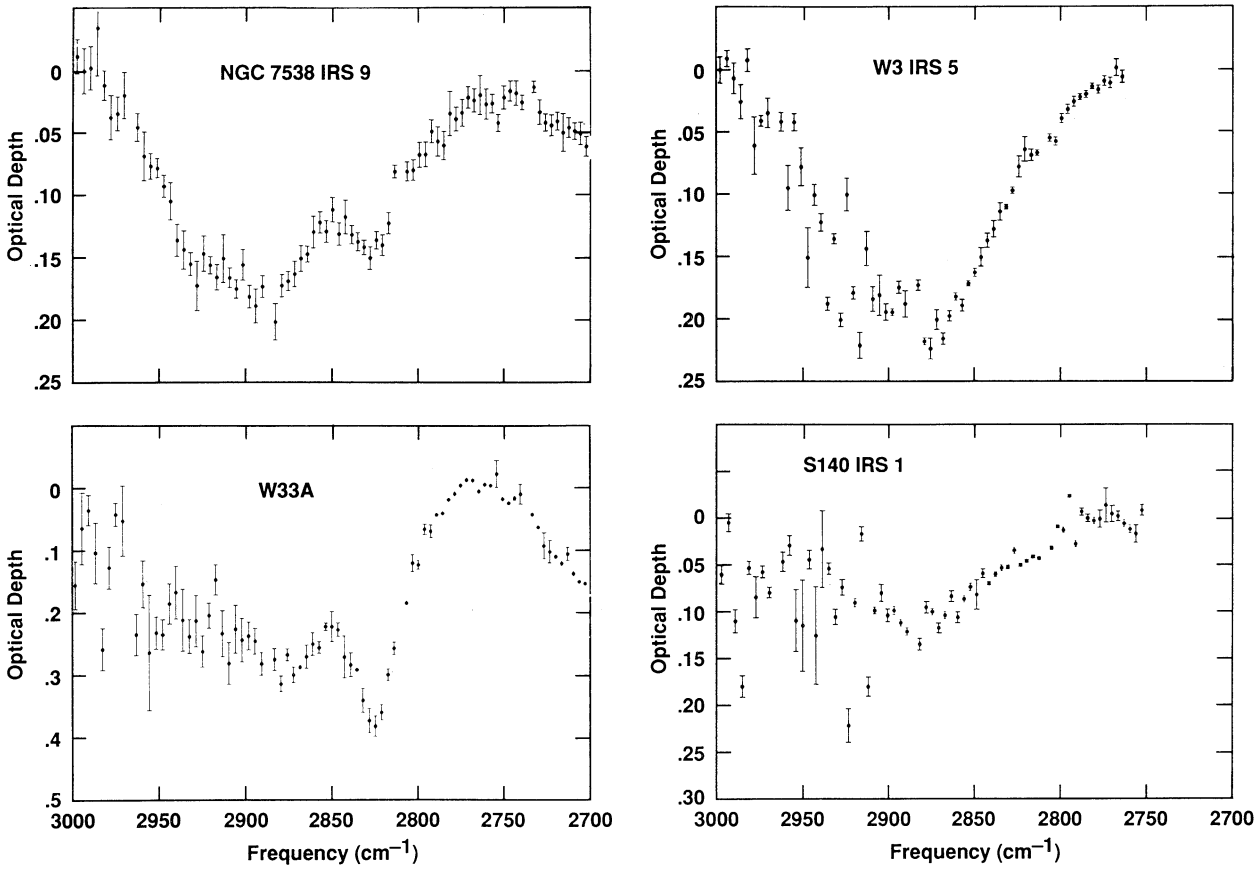

FIG. 3.—High-resolution ($\nu/\Delta\nu \sim 800$ at 3000 cm^{-1}) optical depth spectra in the C–H stretching region for NGC 7538 IRS 9, W33A, W3 IRS 5, and S140 IRS 1. Absorption features peaking near 2825 and 2880 cm^{-1} (3.54 and 3.47 μm) are evident. These features are superposed on the low-frequency wing of the deep O–H stretch band. The baselines used to construct these spectra are shown in Fig. 2. The low single points between 3000 and 2900 cm^{-1} in several of the spectra are due to telluric methane.

frozen in an H_2O–rich ice rather than in pure form. The 2540 cm^{-1} (3.94 μm) component was initially attributed to H_2S because of the close match in peak position to the S–H stretch band in this molecule (Geballe et al. 1985). However, this assignment was based on a narrower range of data which spanned only the 2540 cm^{-1} component. H_2S cannot reproduce both subpeaks, their relative intensities, or profiles.

Formaldehyde (H_2CO) is another potential contributor to the 2825 cm^{-1} (3.54 μm) band. It is readily produced in all interstellar ice analogs containing C, O, and H irradiated by ultraviolet photons or energetic particles (Hagen, Allamandola, & Greenberg 1979; Hagen 1982; Moore et al. 1983; Schutte 1988; Allamandola, Sandford, & Valero 1988), and interstellar chemistry models predict that it should be abundant on grains (Tielens & Hagen 1982; d'Hendecourt et al. 1985). In CO or CO_2–rich mixed molecular ices at 10 K, the asymmetric and symmetric C–H stretch bands of H_2CO peak at 2900 and 2837 cm^{-1} (3.448 and 3.525 μm), respectively (van der Zwet et al. 1985), and in H_2O–rich ices with H_2CO concentrations on the order of a few percent, the corresponding bands fall at 2885 and 2825 cm^{-1} (3.466 and 3.540 μm) (Schutte, Allamandola, & Sandford 1992). Thus, the 2825–2835 cm^{-1} symmetric C–H stretch of H_2CO could contribute to the interstellar 2825 cm^{-1} feature. However, the integrated absorbance of this H_2CO band is only slightly larger than that of its partner. In view of the prominence of the 2825 cm^{-1} band in the spectrum of W33A and the absence of a well-defined feature with comparable strength centered near 2900 cm^{-1}, we conclude that formaldehyde is not an important ice constituent toward this object, in agreement with the conclusions drawn by Grim et al. (1991). At most, it could be present at a level of a few percent of that of the H_2O. The absence of a well-defined band at 2825 cm^{-1} (3.54 μm) in the spectra of W3 IRS 5 and S140 IRS 1 shows that formaldehyde can only be a very minor component toward these objects, if present at all, and that the 2880 cm^{-1} (3.47 μm) band in the spectra of all four objects does not arise from formaldehyde. For NGC 7538 IRS 9 the abundance of H_2CO is difficult to assess because of the deep 2880 cm^{-1} band. A better observational test for H_2CO may be provided by the carbonyl (C=O) stretch which calls at 1720 cm^{-1} (5.81 μm) in these solids and absorbs about 4 times as strongly as the C–H stretching bands. Low-resolution spectra of W33A and NGC 7538 IRS 9 in the 2000–1250 cm^{-1} (5–8 μm) region place H_2CO at the 0.5% level with respect to H_2O in grain mantles (Tielens & Allamandola 1987).

Earlier conclusions that CH_3OH is an important interstellar ice component were based on the good match between the interstellar 1460 cm^{-1} (6.85 μm) band profile and position in the spectra of NGC 7538 IRS 9, W33A, and W3 IRS 5 with the laboratory spectrum of CH_3OH in H_2O at 10 K (Tielens & Allamandola 1987). Thus, finding confirming spectroscopic evidence for CH_3OH in the C–H stretch region toward NGC 7538 IRS 9 and W33A is not surprising. The lack of a similarly clear CH_3OH absorption band toward W3 IRS 5 or S140 IRS

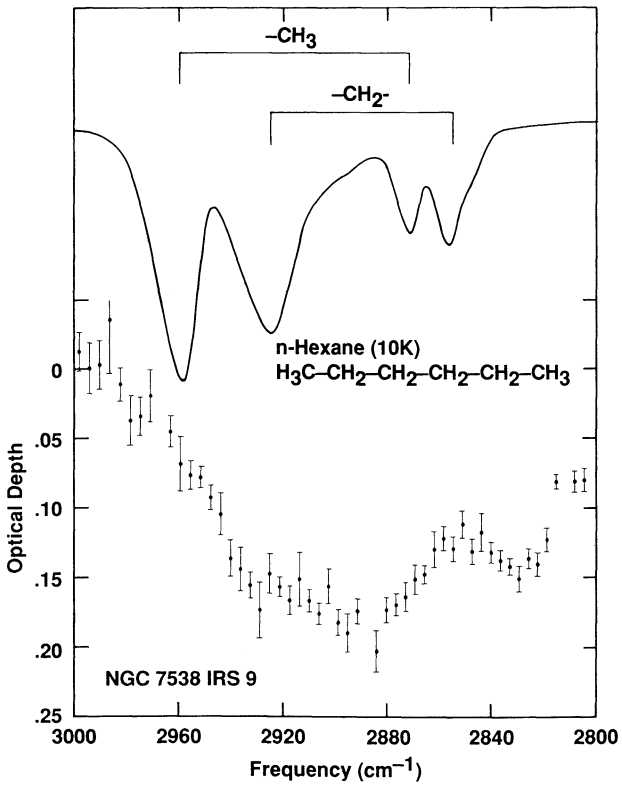

FIG. 4.—Optical depth spectrum of NGC 7538 IRS 9 in the C–H stretch region, compared with that of a saturated, aliphatic hydrocarbon *n*-hexane ice ($H_3C–CH_2–CH_2–CH_2–CH_2–CH_3$) at 10 K. This comparison demonstrates that saturated aliphatic hydrocarbons are not responsible for this spectral structure superposed on the O–H band of this object.

1 is probably due to lower ice column densities [τ-values of the 3250 cm^{-1} (3.08 μm) OH band are 4.6, >7.0, 3.0, and 1.3 for NGC 7538 IRS 9, W33A, W3 IRS 5, and S140 IRS 1, respectively (Capps et al. 1978; Willner et al. 1982)] coupled with uncertain baselines, scattering, and line blending with the strong 2880 cm^{-1} feature.

4.2. *Methanol Column Density Determinations*

The column density, N (molecules cm^{-2}), of an infrared absorbing material is determined from

$$N = \frac{1}{A}\int \tau(\nu)d\nu \approx \frac{1}{A}\,\tau_{\max}\,\Delta\nu_{1/2}\,, \qquad (2)$$

where τ is the optical depth, $\Delta\nu$ is the full width at half-height in inverse centimeters, and A is the integrated absorbance in centimeters per molecule (e.g., d'Hendecourt & Allamandola 1986).

In the C–H stretch region, the overlap with the low-frequency side of the broad and deep interstellar O–H stretch feature produces baseline ambiguity resulting in significant uncertainties in derived column densities as well as band profiles. We have chosen a linear baseline from 3000 to 2770 cm^{-1} (3.33–3.61 μm), the approximate endpoints of the interstellar absorption feature superposed on the wider low-frequency wing which extends from about 3125 to 2670 cm^{-1} in the spectra of protostars (Smith et al. 1989). This baseline choice eliminates the underlying wing, *but does not alter substructure peak positions by more than* 5 cm^{-1}, *since these are much narrower* (10–30 cm^{-1}) *than the underlying wing itself, which spans about* 450 cm^{-1}. This is a conservative baseline and results in an underestimate of the band strengths, since the underlying absorption due to the O–H stretching mode should be concave downward in this region. An alternative approach would be to extend the broad O–H band peaking at 3250 cm^{-1} (3.08 μm) and long-wavelength wing, drawing in what it would be expected to look like if there were no hydrocarbon bands present. Smith et al. (1989) have taken such an approach in analyzing low-resolution ($\nu/\Delta\nu = 160$) spectra, generally using the spectrum of amorphous, solid H_2O to construct the baseline across the entire interstellar O–H stretch band. Their residual, then, consists of all possible contributors to the wing, such as blended hydrocarbon bands and acid-base interactions. They favor an explanation in blended hydrocarbon bands such as are produced by a char. Accounting for the entire wing with acid-base interactions requires a base concen-

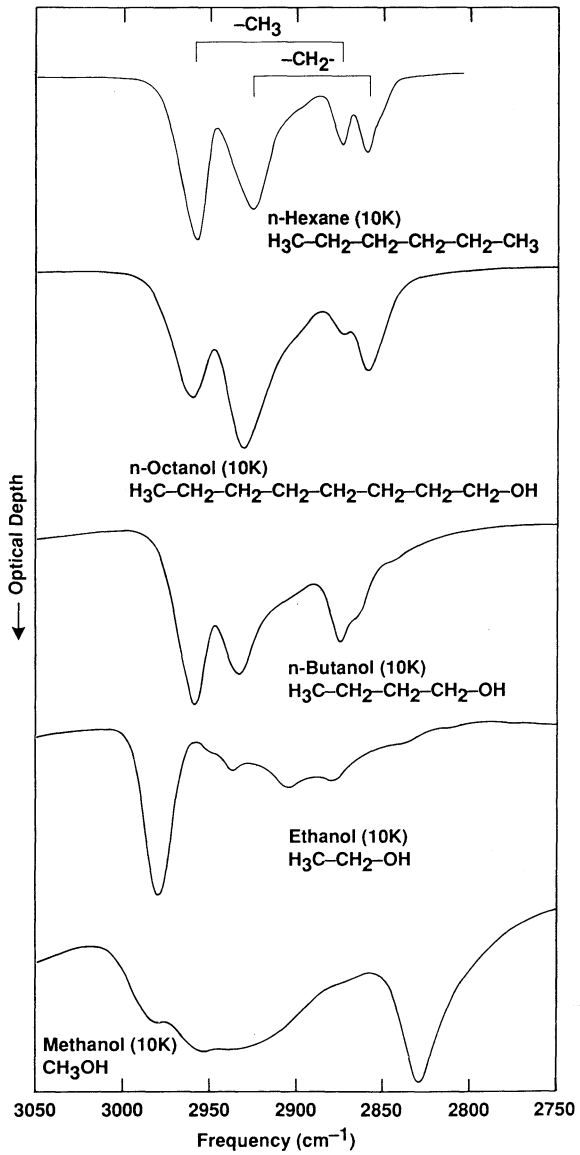

FIG. 5.—Absorbance spectra of several alcohols and *n*-hexane at 10 K in the C–H stretch region, showing the unique spectral signature of the simpler alcohols. As aliphatic chain length increases, the influence of the OH group diminishes and the spectra begin to resemble those of aliphatic hydrocarbons.

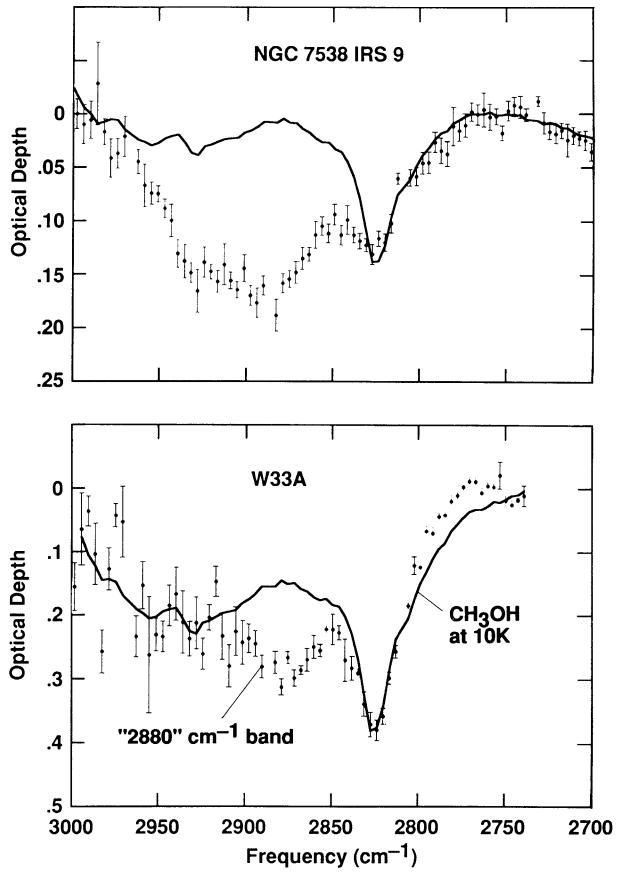

FIG. 6.—Optical depth spectra of NGC 7538 IRS 9 and W33A in the C–H stretch region compared with that of a methanol (CH_3OH) ice at 10 K. This comparison shows that methanol is responsible for the 2825 cm^{-1} (3.54 μm) interstellar band and contributes some absorption to the broad feature between about 3000 and 2850 cm^{-1} as well. To construct a self-consistent methanol optical depth spectrum, we chose baseline limits of 3000 and 2770 cm^{-1} for the laboratory spectrum (the same values used for the interstellar spectra.).

tration on the order of 20%–30%. Constructing a baseline in this way (as compared with the linear baseline we use) would not change substructure peak positions, but would tend to increase the depth of the hydrocarbon bands from about 3000 to 2850 cm^{-1} (3.33–3.51 μm), with the bands in the 2950–2850 cm^{-1} (3.39–3.51 μm) region most affected. Some justification for such an approach can be obtained by comparing this region of the spectrum of pure CH_3OH at 10 K with that of H_2O:CH_3OH (d'Hendecourt & Allamandola 1986) and H_2O:CH_3OH:CO:NH_3 mixtures, before and after UV irradiation (Allamandola et al. 1988). Although the methanol C–H stretching vibrations produce a broad, intense feature centered at roughly 2850 cm^{-1} (3.51 μm) in addition to the narrower 2825 cm^{-1} (3.54 μm) band, the former appears insignificant in the mixture because it blends with the broader, more strongly absorbing H_2O feature. In the far more complex interstellar case, baseline uncertainty is further complicated by the probable presence of other hydrocarbons which could also blend with this band. Much of the uncertainty in the influence of the baseline on the derived column densities can be dealt with by adopting the same baseline endpoints in the laboratory spectra. This is particularly true for the narrower 2825 cm^{-1} feature. Our adopted procedure results in reasonably accurate peak positions and *firm* lower limits to the column densities. We estimate that the column densities could be at most 30% larger for W33A, 50% larger for NGC 7538 IRS 9, and, at most a factor of 2 greater for W3 IRS 5 and S140.

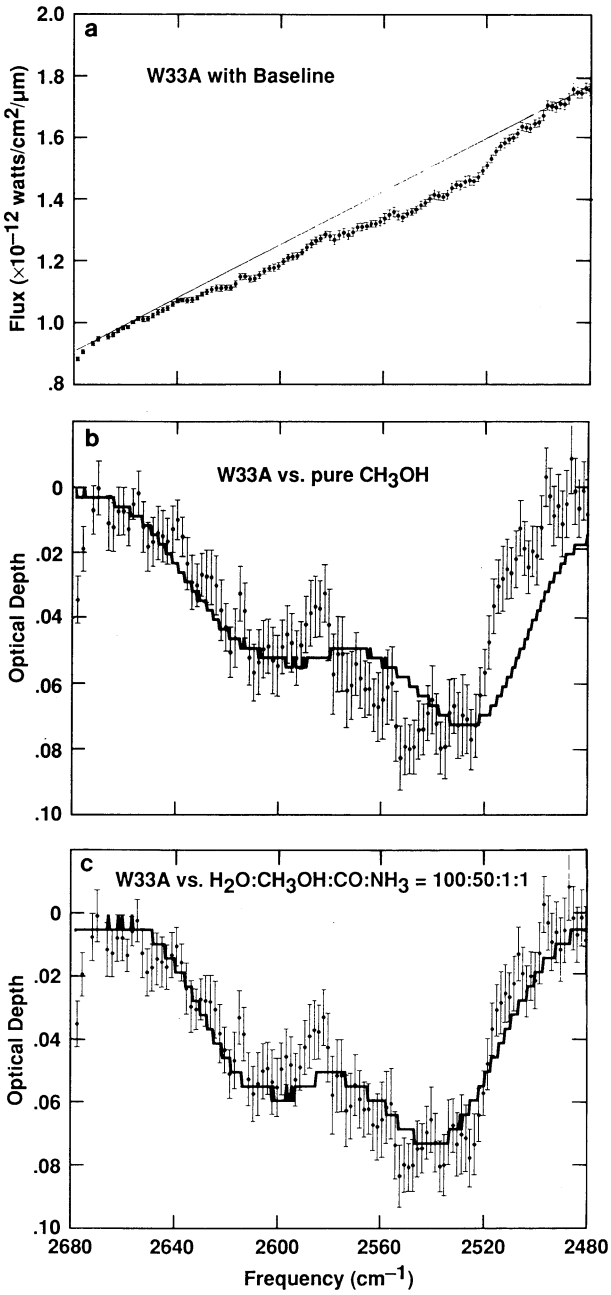

FIG. 7.—The 2680–2480 cm^{-1} (3.73–4.03 μm) spectrum of W33A compared with that of pure methanol (CH_3OH) and methanol-containing ices at 10 K. (*a*) Spectrum of W33A (adapted from Geballe 1991) and the baseline used to construct the optical depth plots in (*b*) and (*c*). (*b*) Optical depth spectrum of W33A compared with that of pure methanol ice at 10 K. (*c*) Optical depth spectrum of W33A compared with that of an H_2O:CH_3OH:NH_3:CO = 100:50:1:1 astrophysical ice analog at 10 K. The spectral behavior of the laboratory ice (*solid line*) in this region is due to methanol. The comparisons in (*b*) and (*c*) show that methanol can account for this interstellar band pair. The better fit in (*c*) suggests that the methanol is intimately mixed in an H_2O–rich ice rather than frozen as an unmixed, pure component.

TABLE 2

SPECTRAL CHARACTERISTICS AND COLUMN DENSITIES OF THE 2825 cm^{-1} CH_3OH AND "2880" cm^{-1} HYDROGENATED INTERSTELLAR "DIAMOND" ABSORPTION BANDS

	"Diamond" Band: 2880 cm^{-1} (3.47 μm)	Methanol Band: 2825 cm^{-1} (3.54 μm)[a]
NGC 7538 IRS 9		
ν (cm^{-1})	2885	2825
τ	0.18	0.13
$\Delta\nu$ (cm^{-1})	85	28
$\tau\Delta\nu/A$ (molecules cm^{-2})	3.8×10^{18} [b]	9.1×10^{17} [c]
W33A		
ν (cm^{-1})	2880	2825
τ	0.15	0.39
$\Delta\nu$ (cm^{-1})	40	40
$\tau\Delta\nu/A$ (molecules cm^{-2})	1.5×10^{18} [b]	4.0×10^{18} [c]
W3 IRS 5		
ν (cm^{-1})	2875	[2825]
τ	0.14	[0.07]
$\Delta\nu$ (cm^{-1})	80	[30]
$\tau\Delta\nu/A$ (molecules cm^{-2})	2.8×10^{18} [b]	[5.3×10^{17}][c]
S140 IRS 1		
ν (cm^{-1})	2885	[2825]
τ	0.14	[0.05]
$\Delta\nu$ (cm^{-1})	80	[30]
$\tau\Delta\nu/A$ (molecules cm^{-2})	2.8×10^{18} [b]	[3.8×10^{17}]

[a] The numbers in brackets are upper limits derived assuming that the entire absorption at 2825 cm^{-1} is due to methanol.

[b] Calculated using A (per C–H) = 4×10^{-18} cm $molecule^{-1}$ measured for tertiary carbon (Wexler 1967).

[c] Calculated using A (CH_3OH, 2825 cm^{-1}) = 4×10^{-18} cm $molecule^{-1}$ (d'Hendecourt & Allamandola 1986). This is for a H_2O:CH_3OH = (2:1) 10 K ice. This value is accurate to within 20% of that measured in H_2O:CH_3OH mixtures in the 10:1 to 2:1 range. For pure CH_3OH, $A = 7.6 \times 10^{-18}$ cm $molecule^{-1}$ (d'Hendecourt & Allamandola 1986).

The measured optical depths and bandwidths used, and the column densities derived from the spectra in Figure 3, are listed in Table 2. These column densities are compared with those of other grain components in Table 3, including CH_3OH column densities determined from the 1460 cm^{-1} (6.85 μm) C–H deformation band, and for W33A, the weaker doublet at 2600 and 2540 cm^{-1} (3.85 and 3.94 μm).

The observed CH_3OH/H_2O ratio determined from the 2825 cm^{-1} (3.54 μm) CH_3OH band and the 3250 cm^{-1} (3.08 μm) H_2O band is 0.13 for NGC 7538 IRS 9. For W33A, the depth of the 3250 cm^{-1} (3.08 μm) band has not been detected. Comparing the observed profile of this band (Capps et al. 1978; Grim et al. 1991) with that of NGC 7538 IRS 9 and profiles reported by Smith et al. (1989), an optical depth of 5.3 is estimated. Using this value, the column density listed in Table 3 is calculated, and a CH_3OH/H_2O ratio of 0.4 is then deduced for W33A. Assuming that all the absorption at 2825 cm^{-1} in the spectrum of W3 IRS 5 and S140 IRS 1 is due to methanol, CH_3OH/H_2O ratios of less than 0.09 and less than 0.18 are obtained. These abundance ratios are typically (except for W33A) much less than those derived from the 1460 cm^{-1} (6.85 μm) CH_3OH deformation mode and the 1665 cm^{-1} (6.0 μm) H_2O scissoring mode measured for these sources (i.e., $CH_3OH/H_2O \approx 0.50$; Tielens & Allamandola 1987).

It should be emphasized, however, that all column densities (i.e., H_2O and CH_3OH) derived from absorption features in the 3 μm region tend to be less than those derived from the 6 μm region. This is particularly true for W33A. It is therefore not surprising that Grim et al. (1991) derived a much lower CH_3OH/H_2O ratio ($\sim$0.1) from the ratio of the 2825 cm^{-1} to the 1665 cm^{-1} bands. The CH_3OH/H_2O ratios determined from the 1460 cm^{-1} (6.85 μm) and 1665 cm^{-1} (6.00 μm) bands are 0.61, 0.54, and 0.81, as compared with 0.13, 0.4, and 0.09 derived above for NGC 7538 IRS 9, W33A, and W3 IRS 5, respectively. The decrease in the CH_3OH/H_2O ratio derived in going from the 3 μm to the 5–8 μm regions of the spectra in

TABLE 3

DERIVED COLUMN DENSITIES (molecules cm^{-2}) OF INTERSTELLAR DUST COMPONENTS COMPARED WITH HYDROGEN

MATERIAL	OBJECT			
	NGC 7538 IRS 9	W33A	W3 IRS 5	S140 IRS 1
Hydrogen[a]	1.6×10^{23}	2.8×10^{23}	2.7×10^{23}	1.4×10^{23}
CH_3OH:				
2825 cm^{-1} [b]	9.1×10^{17}	3.9×10^{18}	$<5.3 \times 10^{17}$	$<3.8 \times 10^{17}$
2600 + 2540 cm^{-1} [c]	...	2.5×10^{18}	...	...
1460 cm^{-1} [d]	6.7×10^{18}	2.3×10^{19}	3.5×10^{18}	...
H_2O:				
3250 cm^{-1} [e]	7×10^{18}	9×10^{18}	5.8×10^{18}	2.1×10^{18}
1665 cm^{-1} [d]	1.1×10^{19}	4.2×10^{19}	4.3×10^{18}	8.8×10^{18}
CO (nonpolar ice)[f]	6.4×10^{17}	1.1×10^{17}	1.1×10^{17}	...
CO (polar ice)[f]	3.2×10^{17}	2.8×10^{17}	5.4×10^{16}	...
CO (gas)[f]	1.4×10^{19}	2.0×10^{19}	2.2×10^{19}	...
"Diamonds"[b]	3.8×10^{18}	1.5×10^{18}	2.8×10^{18}	2.8×10^{18}

[a] From $N_H = 1.9 \times 10^{21} A_V$.

[b] This work.

[c] This work and Geballe 1991; assuming $A = 2.6 \times 10^{-18}$ cm $molecule^{-1}$, appropriate for a H_2O:CH_3OH = 2:1 10 K ice.

[d] Tielens & Allamandola 1987.

[e] NGC 7538 IRS 9 by matching the spectrum in Fig. 1 with those from Smith et al 1989; W33A by matching the high-frequency side of the O–H band with those in Smith et al. 1989; W3 IRS 5 from Smith et al. 1989; S140 IRS 1 from Willner et al. 1982.

[f] Tielens et al. 1991.

these same sources reflects, then, a proportionally larger decrease in the CH_3OH column density than in the H_2O column density in going to the higher frequencies. It is likely, as suggested by Pendleton, Tielens, & Werner (1990), in their study of infrared reflection nebulae around protostars showing bipolar geometries, that the 3 μm photons "leak" out through the poles of a flattened dust distribution, while those in the 6 μm region traverse the disk. Thus, the photons in the 3 μm region probe a smaller dust column density than those in the 6 μm region. If this picture is correct, the CH_3OH/H_2O ratio has to be higher in the disk than in the general dense cloud medium. The observed high variability in the CH_3OH/H_2O ratio from source to source in the 3 μm region versus the relative consistency of these ratios in the 6 μm region lends some support to this possibility. Alternatively, as pointed out by Grim et al. (1991), the 1460 cm^{-1} (6.85 μm) band might be largely due to species other than CH_3OH. Among the proposed identifications are NH_4^+ (Grim et al. 1991) in photolyzed grain mantles and carbonates (Sandford & Walker 1985). This issue has been reviewed by Tielens & Allamandola (1987) and Tielens (1989). Here we merely point out that the resolution of this critical issue will have to await higher spectral resolution studies of the 1460 cm^{-1} (6.85 μm) interstellar band toward several objects.

4.3. *The* 2880 cm^{-1} (3.47 μm) *Band and Interstellar Diamonds*

An unexpected result of these observations is the discovery of a prominent new interstellar band at 2880 cm^{-1} (3.47 μm). Figure 8 compares the optical depth spectrum of S140 IRS 1 with the residual optical depth of NGC 7538 IRS 9, W33A, and W3 IRS 5 remaining after subtraction of the methanol component shown in Figure 6. The derived shape of this new band is somewhat uncertain in the spectra of NGC 7538 IRS 9 and W33A owing to the overlap with the broad 2950 cm^{-1} CH_3OH feature and the uncertainty in the adopted continuum. The 2880 cm^{-1} feature in W3 IRS 5 and S140 is much less affected by this; but note the strong telluric and interstellar gas-phase CH_4 absorption around 2950 cm^{-1} in these spectra.

The new band occupies a unique position in the aliphatic C–H stretch spectral region. Absorptions falling near 2890 cm^{-1} (3.46 μm) are characteristic of tertiary C–H stretching vibrations (Bellamy 1958; Silverstein & Bassler 1967). We tentatively assign the interstellar 2880 cm^{-1} band to this chemical group. A tertiary aliphatic carbon is one in which three of its four single, covalent (sp^3) bonds are to carbon atoms, while the remaining one is to a species other than carbon, such as hydrogen (Morrison & Boyd 1966). A secondary aliphatic carbon is one in which two of its four single bonds are to carbon atoms and two to other species, and a primary aliphatic carbon is one in which only one of the four bonds is to carbon. Hydrogen atoms attached to these different classes of carbon atoms are similarly designated. These different bonding arrangements are illustrated in Figure 9.

Since the integrated absorbances per C–H bond are comparable for primary, secondary, and tertiary carbons (Wexler 1967), the predominance of the 2880 cm^{-1} (3.47 μm) tertiary

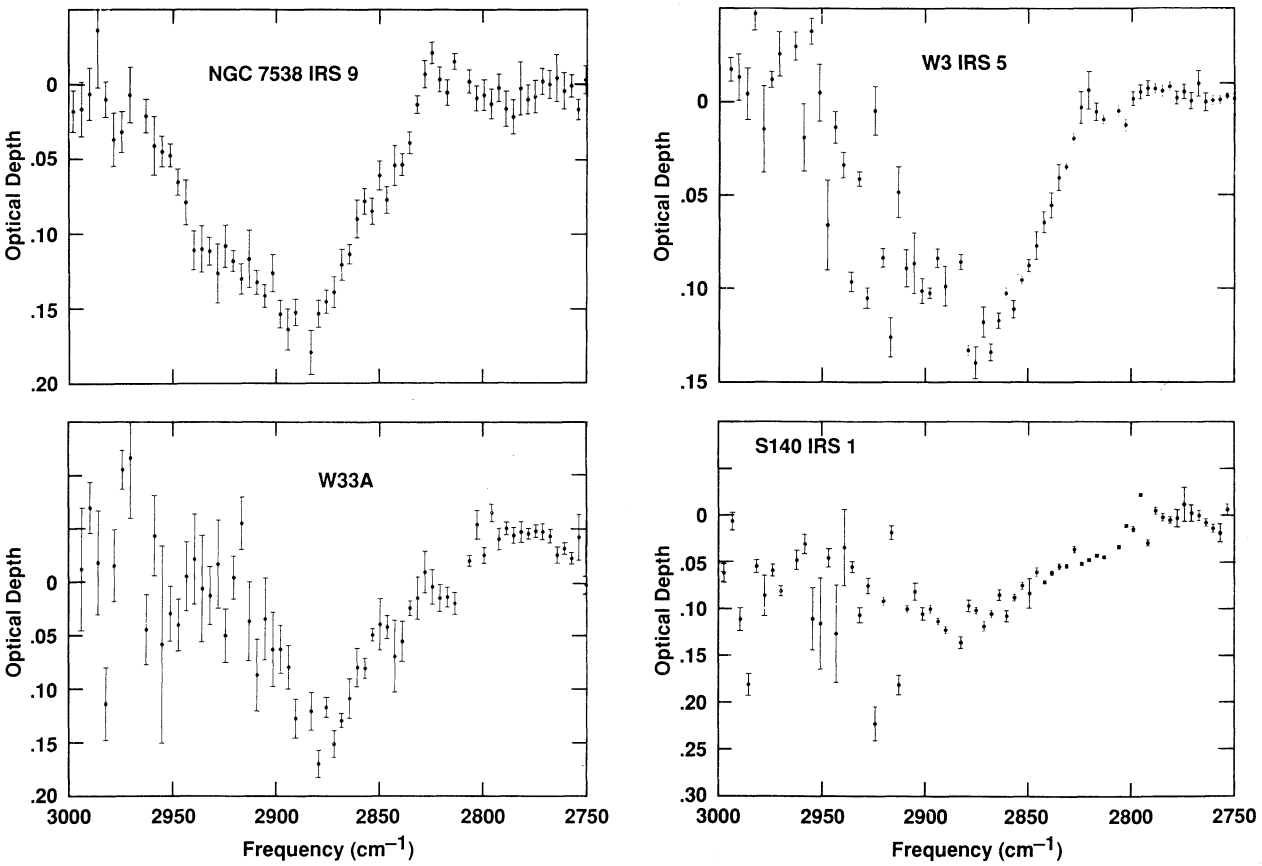

FIG. 8.—Optical depth spectra of the new interstellar 2880 cm^{-1} (3.47 μm) band. For NGC 7538 IRS 9 and W33A, the residual optical depths remaining after the removal of the methanol contributions shown in Fig. 6 are given. For W3 IRS 5 the residual optical depth was derived by subtracting a methanol optical depth spectrum assuming that all of the absorbance at 2825 cm^{-1} is due to CH_3OH. The spectrum of S140 IRS 1 is the same as that shown in Fig. 3.

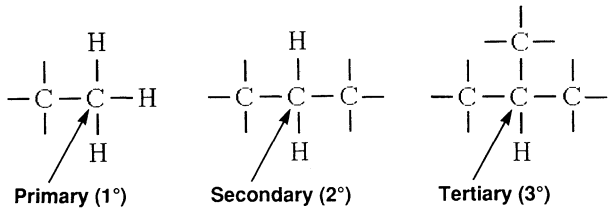

FIG. 9.—The three classes of carbon in aliphatic hydrocarbons. Each has highly characteristic C–H stretching frequencies. Hydrogen atoms are similarly designated as 1°, 2°, or 3°, depending on the class of the carbon atom to which it is attached.

band places significant constraints on the structure of the hydrocarbons in dense molecular clouds. If there were equal numbers of primary, secondary, and tertiary hydrogenated carbon atoms in the interstellar material giving rise to the absorption in the C–H stretching region superposed on the low-frequency wing of the H_2O feature, there would be bands at about 2960 primary, $-CH_3$, 2925 (secondary, $-CH_2-$), 2880 $\left(\text{tertiary, } -\overset{|}{C}H\right)$, 2870 (primary, $-CH_3$), and 2860 (secondary, $-CH_2-$) cm^{-1} (3.38, 3.42, 3.47, 3.48, and 3.50 μm), with relative intensities of about 3:2:1:0.6:0.6, respectively. Figure 8 shows that this is not the case. If we attribute the absorption at these frequencies solely to primary, secondary, and tertiary carbon groups, the spectra in Figure 8 indicate that there are at least 10 more tertiary carbon-hydrogen bonds in the interstellar material than primary, and there are at least three more tertiary carbon-hydrogen bonds than secondary (3°:2°:1° = 10:3:1). This value of 3 is determined primarily from the spectrum of NGC 7538 IRS 9, the only spectrum with sufficient signal-to-noise to detect a possible shoulder near 2925 cm^{-1}, the position associated with secondary carbon and hydrogen atoms. The *smallest* molecular structure that can satisfy these requirements must contain more than about 30 carbon atoms. Figure 10 shows an example of an atomic arrangement that satisfies these ratios. It is clear from Figure 10 that the only way this can be achieved is if the hydrocarbon in dense molecular clouds is made up mainly of sp^3 hybridized carbon atoms which are bound to one another and hydrogenated on the surface. This is the diamond structure of carbon.

We therefore tentatively attribute this new feature to interstellar diamonds. The detection of this band in the spectra of all four dense molecular clouds we have observed suggests that the carrier is a ubiquitous component in these objects. The variation with respect to the CH_3OH band suggests that this interstellar grain component is probably associated with the refractory carbonaceous grain population rather than with the ices. Realizing that one infrared band is insufficient for an assignment, we will refer to this feature either as the 2880 cm^{-1} band or the "diamond" band. In addition to a C–H stretch band, diamonds will also have a weak C–H bending fundamental near 1340 cm^{-1} (7.46 μm; Bellamy 1958). Very weak C–C stretching fundamentals also fall near this position. The intensity of the stretching mode is increased if some atoms other than carbon (such as oxygen or nitrogen) are also present in the carbon skeleton. In this respect, it is interesting to note that Lacy et al. (1991) report the detection of a weak feature ($\tau = 0.14$) at 1352 cm^{-1} (7.396 μm) in the spectrum of W33A. They do not present spectra in this region for the other sources discussed here.

Recently, small carbon clusters referred to as microdiamonds were detected in oxidized acid residues from several carbonaceous meteorites (Lewis et al. 1987). Isotopic anomalies associated with noble gases in these diamonds point to an interstellar dust origin. This discovery prompted much theoretical discussion of the source of these diamonds. Possibilities considered include carbon star ejecta, interstellar shocks (a high-pressure route) (Tielens et al. 1987; Blake et al. 1988), and several low-pressure mechanisms (Hecht 1987; Nuth 1987). The implications for the assignment of the new 2880 cm^{-1} band to diamonds and their relationship to meteoritic diamonds is discussed in more detail elsewhere (Allamandola et al. 1992).

This new interstellar band, which we tentatively ascribe to hydrogen bonded to the faces of interstellar diamond particles, falls at about 2880 cm^{-1} (3.47 μm), at the limit of the 2890 $\pm$ 10 cm^{-1} range for tertiary C–H stretches in simple hydrocarbons. Uncertainty in the astronomical continuum produces an uncertainty in the peak position of at most 10 cm^{-1}, and it will be important to measure this feature along several other lines of sight with equal or better spectral resolution to characterize it fully and determine its peak position more accurately.

The column densities of the band carrier, calculated using the measured integrated absorbance value A, per C–H (Wexler 1967), are listed at the bottom of Table 3. Abundances,

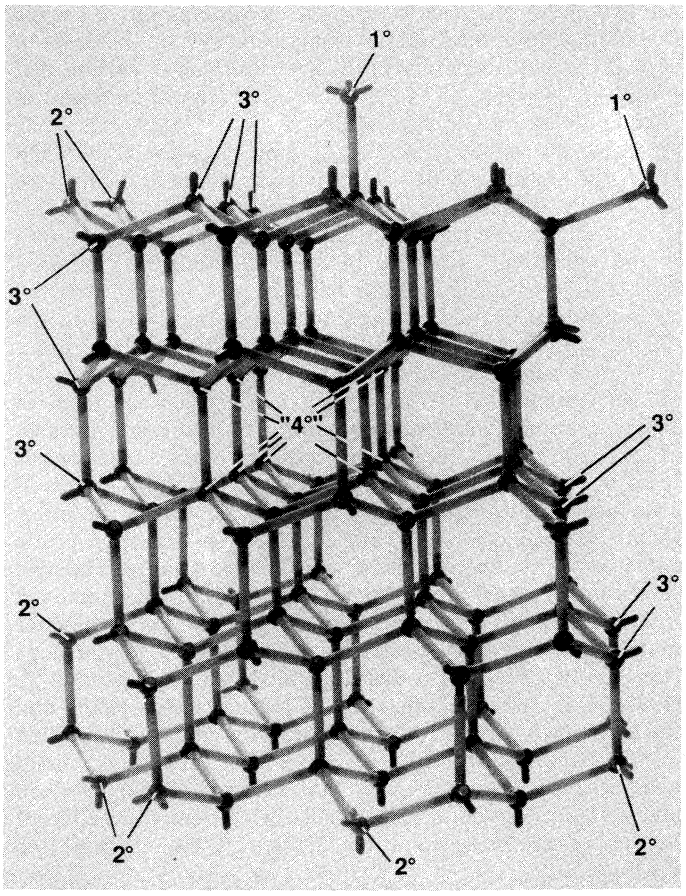

FIG. 10.—Photograph of a molecular model which satisfies the constraints on the relative number of primary (1°), secondary (2°), and tertiary (3°) hydrogen atoms implied by the profile of the 2880 cm^{-1} interstellar band. The only way in which tertiary carbon atoms can dominate the spectrum is if the carbon atoms are arranged in this form, which is the diamond structure of carbon.

TABLE 4

A_V, $\tau_{silicate}$, H AND C COLUMN DENSITIES, AND THE LOWER LIMIT TO THE PERCENT OF COSMIC CARBON IN THE INTERSTELLAR "DIAMONDS"

Object	A_V[a]	$\tau_{silicate}$	$\tau_{diamond}$	N(H)[b]	N(C)[c]	N(CH) "Diamond"	%C[d]
NGC 7538 IRS 9	84	4.5	0.18	1.6×10^{23}	5.9×10^{19}	3.8×10^{18}	6.4
W33A	145	7.8	0.15	2.8×10^{23}	1×10^{20}	1.5×10^{18}	1.5
W3 IRS 5	142	7.6	0.14	2.7×10^{23}	1×10^{20}	2.8×10^{18}	2.8
S140 IRS 1	74.1	4.0	0.14	1.4×10^{23}	5.2×10^{19}	2.8×10^{18}	5.4

[a] From $\tau_{silicate} = A_V/18.6$.
[b] From $N(H) = 1.9 \times 10^{21}/A_V$.
[c] From cosmic C/H = 3.7×10^{-4}.
[d] This does not include the internal carbon atoms.

A_V, $\tau_{silicate}$, the hydrogen and carbon column densities, and the percent of cosmic carbon tied up in the tertiary carbon component are listed in Table 4. Only a lower limit can be placed on the amount of carbon tied up in the carrier of the 2880 cm^{-1} band. This is because the relative amounts of absorption due to primary, secondary, and tertiary carbon and hydrogen atoms probe only those carbon atoms which are bonded to hydrogen, not those which are bonded to four other carbon (or other) atoms. Thus it is possible to increase the number of internal carbon atoms essentially indefinitely within the bounds of cosmic abundance constraints. The final column of Table 4 shows that the lower limit to the amount of cosmic carbon tied up in the form of tertiary carbon is on the order of several percent. Estimates of the total fraction of carbon tied up in the 2880 cm^{-1} (3.47 μm) band carrier can be found in Allamandola et al. (1992).

Taking the values of A_V, $\tau_{silicate}$, and τ_{2880} for NGC 7538 IRS 9, the object for which we have the best data listed in Table 4, we find that $A_V/\tau_{2880} = 470$ and $\tau_{silicate}/\tau_{2880} = 25$. This relationship can be used to estimate the expected contribution of the "diamond" band to the general interstellar infrared extinction, provided that the band carrier is not restricted solely to dense clouds. For example, since the A_V toward the Galactic center is about 30, "diamonds" may contribute about 0.06 to the measured τ of about 0.1 at 2880 cm^{-1} (Sandford et al. 1991). Similarly, for VI Cygnus No. 12, which has an A_V of 10, the diamond band can account for 0.02 of the 0.025 τ-value at 2880 cm^{-1}. Thus, the possible presence of the carrier of this band in the general diffuse ISM is consistent with observed absorbances. This is illustrated in Figure 11, where the interstellar "diamond" band profile, scaled to the appropriate value of A_V, has been plotted with the spectrum of Galactic center source IRS 7. If the "diamond" band profile is removed from the Galactic center spectrum, the residual makes a better match with laboratory spectra of some aliphatic hydrocarbons (see Fig. 4). This point is discussed further in Pendleton et al. (1992). Note, however, that the $-CH_3$ to $-CH_2-$ ratios and the amount of carbon in the hydrocarbon component of dust in the diffuse ISM derived by Sandford et al. (1991) remain valid because they were based on the 2955 and 2930 cm^{-1} (3.38 and 3.41 μm) aliphatic components, which are little affected by the possible presence of the 2880 cm^{-1} (3.4 μm) band (see Fig. 11).

4.4. *Open Questions and Speculations*

The smallest members of the interstellar aromatic hydrocarbon family dominate the infrared emission in the 3 μm region observed from many interstellar objects (Allamandola, Tielens, & Barker 1989; Puget & Léger 1989). In some sources, a minor emission band is present at 2890 cm^{-1} (3.46 μm), very close to the position of the new interstellar feature. This is one of the few emission bands whose assignment has remained ambiguous within the framework of the polycyclic aromatic hydrocarbon (PAH) hypothesis (Barker, Allamandola, & Tielens 1987; Allamandola et al. 1989; Sandford 1991). Exceptionally stable compounds such as diamonds are good candidates as possible contributors to this band, since they could survive the rigors of the emission environments. Thus, if microdiamonds are indeed the carriers of the new interstellar absorption feature, they may also be responsible for the weak 2880 cm^{-1} (3.46 μm) emission band, and their C–C stretching modes could contribute to the broad, intense 1300 cm^{-1} (7.7 μm) emission feature. The interstellar microdiamonds isolated from meteorites have a measured size distribution which spans the same range as derived for interstellar PAHs; consequently, they would experience very similar IR fluorescent processes upon UV photon absorption. In this picture, the weakness of the 2890 cm^{-1} (3.46 μm) emission feature relative to the 3050 cm^{-1} (3.28 μm) aromatic band in interstellar spectra, coupled with the larger abundance derived for the interstellar diamonds than for the PAHs, implies that the smallest interstellar microdiamonds are typically somewhat larger ($N_C \sim 500$ C atoms) than the smallest PAHs.

The optical depth at 2960 cm^{-1} (3.38 μm) and 2920 cm^{-1}

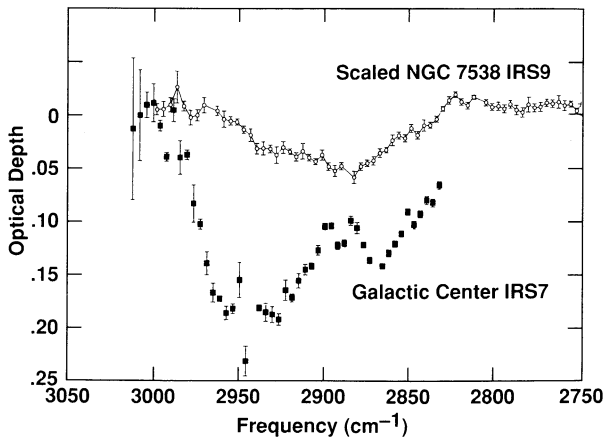

FIG. 11.—Optical depth spectrum of NGC 7538 IRS 9 compared with that of Galactic center source IRS 7. The spectrum of NGC 7538 IRS 9 has been scaled to match an A_V equivalent to that of the Galactic center (see text).

(3.43 μm) allows us to probe the expected contribution of the diffuse medium $-CH_3$ and $-CH_2-$ carrying material toward the objects studied here. Sandford et al. (1991) report $A_V/\tau_{2955} = 310 \pm 90$ and $A_V/\tau_{2925} = 240 \pm 40$. These relationships would predict τ-values of 0.27, 0.47, 0.45, and 0.24 at 2955 cm^{-1}, and 0.35, 0.61, 0.6, and 0.3 at 2925 cm^{-1} toward NGC 7538 IRS 9, W33A, W3 IRS 5, and S140 IRS 1, respectively. These values exceed the observed optical depths in Figures 3 and 6 by factors of 3–10. Perhaps the diffuse medium hydrocarbon component is not present in dense molecular clouds. This is an important issue, and future laboratory work is needed to address this apparent discrepancy.

5. CONCLUSIONS

In this paper high-resolution spectroscopic studies of dense molecular clouds in the 3100–2600 cm^{-1} (3.2–3.9 μm) range are reported. This is the region in which the fundamental C–H stretching vibrations of aliphatic hydrocarbons fall. Two well-resolved absorption bands were detected at about 2825 cm^{-1} (3.54 μm) and 2880 cm^{-1} (3.47 μm). The 2880 cm^{-1} (3.47 μm) band, a new interstellar feature, is moderately strong in the spectra of all four objects studied: NGC 7538 IRS 9, W33A, W3 IRS 5, and S140 IRS 1. The 2925 cm^{-1} (3.54 μm) band, which had been previously detected toward W33A, is also seen in the spectrum of NGC 7538 IRS 9. The variation of the relative strength of these two bands between the different objects indicates they arise from two different carriers.

On the basis of comparisons with laboratory spectra, the 2825 cm^{-1} (3.54 μm) band is assigned to methanol (CH_3OH), in agreement with the earlier work of Grim et al. (1991). This assignment is further supported by the excellent agreement between a pair of weak bands at 2600 and 2540 cm^{-1} (3.85 and 3.94 μm) in the spectrum of CH_3OH and in the high-resolution spectrum of W33A recently reported by Geballe (1991). Comparison of these weak interstellar bands with laboratory data also suggests that the CH_3OH is intimately mixed with the H_2O in the clouds, as opposed to being frozen in its pure form. Thus the presence of CH_3OH ices in dense clouds is confirmed.

The abundances of CH_3OH relative to H_2O for NGC 7538 IRS 9 and W33A, calculated using the observed strengths of the 2825 cm^{-1} methanol band and the 3250 cm^{-1} (3.08 μm) H_2O feature, are 13% and 40%, respectively. These values are smaller than the abundances of 61% and 54% derived using the 1460 cm^{-1} (6.85 μm) band assigned to CH_3OH and the 1665 cm^{-1} (6.00 μm) H_2O band. These apparent discrepancies may be due to a combination of scattering effects within the molecular cloud, uncertainties associated with the baselines for the 2825 cm^{-1} feature, and contributions by other species to the 1460 cm^{-1} (6.85 μm) band. In both cases, after H_2O, methanol is the most abundant interstellar ice constituent known.

The new band at about 2880 cm^{-1} (3.47 μm) falls near the position for C–H stretching vibrations in tertiary carbon atoms $\left(-\overset{|}{\underset{|}{C}}H\right)$. The prominence of this feature, in combination with the lack of strong features associated with primary ($-CH_3$) and secondary ($-CH_2-$) carbon atoms, suggests that the carrier of the new feature has a diamond-like structure. We therefore tentatively attribute this new feature to interstellar "diamonds." The detection of this band in the spectra of all four dense molecular clouds suggests that the carrier is a ubiquitous component of dense clouds. Band-strength analysis indicates that a minimum of a few percent of the available cosmic carbon is tied up in this material. This interstellar grain component is probably associated with a refractory carbonaceous grain component rather than the ices.

On first principles, one would have expected a complex mixture of nearly equally abundant interstellar aliphatic hydrocarbons. If this were the case, their C–H stretching bands would likely suffer severe blending, making peak positions and band profiles difficult to discern. Perhaps this *is* responsible for the bulk of the low-frequency wing of the O–H stretch band. Nonetheless, it seems surprising that such important diagnostic spectroscopic structure as the 2825 cm^{-1} (3.54 μm) and the new 2880 cm^{-1} (3.47 μm) band are evident on the wing. This implies that nature is quite selective in the production of some hydrocarbons.

We thank Tom Geballe for sending us his spectrum of W33A in the 2680–2480 cm^{-1} region prior to publication. We also thank Jeff Lee for helping us measure the alcohol spectra used here, and Ed Anders for a very fruitful discussion concerning the new 2880 cm^{-1} band and meteoritic diamonds. This work was supported by NASA grants 199-52-12-04 and 452-33-93-03.

REFERENCES

Allamandola, L. J. 1984, in Galactic and Extragalactic Infrared Spectroscopy, ed. M. F. Kessler & J. P. Phillips (Dordrecht: Reidel), 5
Allamandola, L. J., Sandford, S. A., Tielens, A. G. G. M., & Herbst, T. 1992, Nature, submitted
Allamandola, L. J., Sandford, S. A., & Valero, G. J. 1988, Icarus, 76, 225
Allamandola, L. J., Tielens, A. G. G. M., & Barker, J. R. 1989, ApJS, 71, 733
Baas, F., Grim, R. J. A., Geballe, T. R., Schutte, W., & Greenberg, J. M. 1988, in Dust in the Universe, ed. M. Bailey & D. A. Williams (Cambridge: Cambridge Univ. Press), 55
Barker, J. R., Allamandola, L. J., & Tielens, A. G. G. M. 1987, ApJ, 315, L61
Bellamy, L. J. 1958, The Infra-red Spectra of Complex Organic Molecules (2d ed.; New York: Wiley)
Blake, D. F., et al. 1988, Nature, 332, 611
Capps, R. W., Gillett, F. C., & Knacke, R. F. 1978, ApJ, 226, 863
d'Hendecourt, L. B., & Allamandola, L. J. 1986, A&AS, 64, 453
d'Hendecourt, L. B., Allamandola, L. J., & Greenberg, J. M. 1985, A&A, 152, 130
Dyck, H. M., & Howell, R. R. 1982, AJ, 87, 400
Eiroa, C., Lenzen, R., & Gomez, A. I. 1988, A&A, 190, 283
Eiroa, C., Lenzen, R., Leinert, C., & Hodapp, K. W. 1987, A&A, 179, 171
Geballe, T. R. 1991, MNRAS, 251, 24
Geballe, T.R., Baas, F., Greenberg, J. M., & Schutte, W. 1985, A&A, 146, L6
Grim, R. J. A., Baas, F., Geballe, T. R., Greenberg, J. M., & Schutte, W. 1991, A&A, 243, 473
Hagen, W. 1982, Ph.D. thesis, Univ. Leiden
Hagen, W., Allamandola, L. J., & Greenberg, J. M. 1979, AP&SS, 65, 215
———. 1980, A&A, 86, L3
Hagen, W., Tielens, A. G. G. M., & Greenberg, J. M. 1983, A&A, 117, 132
Hecht, J. H. 1987, Nature, 328, 765
Hough, J. H., et al. 1988, MNRAS, 230, 107
IRTF Photometry Manual. 1988, comp. A. Tokunaga, Univ. Hawaii
Lacy, J. H., Carr, J. S., Evans, N. J., II, Baas, F., Achtermann, J. M., & Arens, J. F. 1991, ApJ, 376, 556
Léger, A., Gauthier, S., Defourneau, D., & Rouan, D. 1983, A&A, 117, 164
Lewis, R. S., Tang, M., Wacker, J. F., Anders, E., & Steel, E. 1987, Nature, 326, 160
Moore, M. H., Donn, B., Khanna, R., & A'Hearn, M. F. 1983, Icarus, 54, 388
Morrison, R. T., & Boyd, R. N. 1966, Organic Chemistry (Boston: Allyn & Bacon)
Nuth, J. A. 1987, Nature, 329, 589
Pendleton, Y., Sandford, S. A., Allamandola, L. J., Tielens, A. G. G. M., & Sellgren, K. 1992, in preparation
Pendleton, Y., Sandford, S. A., Allamandola, L. J., Tielens, A. G. G. M., & Werner, M. W. 1990, ApJ, 349, 107
Puget, J. L., & Léger, A. 1989, ARA&A, 27, 161
Sandford, S. A. 1991, ApJ, 376, 599
Sandford, S. A., Allamandola, L. J., Tielens, A. G. G. M., Sellgren, K., Tapia, M., & Pendleton, Y. 1991, ApJ, 371, 607
Sandford, S. A., & Walker, R. M. 1985, ApJ, 291, 838
Schutte, W. A. 1988, Ph.D. thesis, Univ. Leiden

Schutte, W., Allamandola, L. J., & Sandford, S. A. 1992, Icarus, submitted
Schutte, W. A., Tielens, A. G. G. M., & Sandford, S. A. 1991, ApJ, 382, 523
Silverstein, R. M., & Bassler, G. C. 1967, Spectrometric Identification of Organic Compounds (New York: Wiley), chap. 3
Skinner, C. L., Tielens, A. G. G. M., Barlow, M. J., & Justtanont, K. 1992, A&A, submitted
Smith, R.G., Sellgren, K., & Tokunaga, A. T. 1987, ApJ, 334, 209
———. 1989, ApJ, 344, 413
Tanaka, M., Sato, S., Nagata, T., & Yamamoto, T. 1990, ApJ, 352, 724
Tielens, A. G. G. M. 1989, in Interstellar Dust, ed. L. J. Allamandola & A. G. G. M. Tielens (Dordrecht: Kluwer), 239
Tielens, A. G. G. M., & Allamandola, L. J. 1987, in Physical Processes in Interstellar Clouds, ed. G. E. Morfill & M. Scholer (Dordrecht: Reidel), 333
Tielens, A. G. G. M., Allamandola, L. J., Bregman, J. D., Goebel, J., d'Hendecourt, L. B., & Witteborn, F. C. 1984, ApJ, 287, 697
Tielens, A. G. G. M., & Hagen, W. 1982, A&A, 114, 245
Tielens, A. G. G. M., Seab, C. G., Hollenbach, D. J., & McKee, C. 1987, ApJ, 319, L103
Tielens, A. G. G. M., Tokunaga, A. T., Geballe, T. R., & Baas, F. 1991, ApJ, 381, 181
Tokunaga, A. T., Smith, R. G., & Irwin, E. 1987, in Infrared Astronomy with Arrays, ed. C. G. Wynn-Williams, E. E. Becklin, & L. H. Good (Honolulu: Univ. Hawaii), 367
van der Zwet, G. P., Allamandola, L. J., Baas, F., & Greenberg, J. M. 1985, A&A, 145, 262
Werner, M. W., Becklin, E. E., Gatley, I., Matthews, K., Neugebauer, G., & Wynn-Williams, C. G. 1979, MNRAS, 188, 463
Wexler, A. S. 1967, Appl. Spectrosc. Rev., 1, 29
Whittet, D. C. B., Bode, M. F., Longmore, A. J., Baines, D. W. T., & Evans, A. 1983, Nature, 303, 218
Willner, S. P., et al. 1982, ApJ, 253, 174